THE IMPLICATION OF ELASTIC DEFORMATION IN WAVE-ICE INTERACTION

LUOFENG HUANG[1], LUKE BENNETTS[2], PHILIP CARDIFF[3], HRVOJE JASAK[4, 5, 6],
ZELJKO TUKOVIC[6], GILES THOMAS[1]

[1]*University College London, UK*   [2]*University of Adelaide, Australia*
[3]*University College Dublin, Ireland*   [4] *Wikki Ltd, London, UK*
[5] *University of Cambridge, UK*   [6]*University of Zagreb, Croatia*

Keywords: Fluid-Structure Interaction, Hydroelasticity, Sea Ice, Ocean Surface Wave, Energy Dissipation

1.   Introduction

Global warming has induced a paradigm change in the Arctic environment, as is evident in the transition from continuous sea ice coverages to broken fields of ice floes separated by open water. The increased open-water area results in increased wave activity, and the waves interact with the broken ice floes. When encountering an ice floe, waves partially pass through and are partially reflected, with the rest of the energy dissipated. Modelling this process is the key to knowing how much energy can be transmitted and how much energy is dissipated, determining how far the waves can propagate as well as potential additional shrinkage of continuous ice coverage due to wave breaking.

Research into this problem started with theoretical and experimental models. In most cases, the ice floe is modelled as a thin elastic plate subjected to regular ocean waves. By predicting or measuring the waves upstream and downstream, the proportion of the reflected and transmitted wave energies can be obtained, expressed as reflection and transmission coefficients (R & T). Within the potential-flow theory that has been most widely applied to this problem, energy dissipation is neglected, thus R + T = 1. However, recent experiments of Bennetts & Williams [1] and Tofolli et al. [2] demonstrated that R + T = 1 may not be the case; the reason is mainly an energy dissipative "overwash" phenomenon. Overwash is defined as waves running over the floe surface, as presented in the experiments of Skene et al. [3], in which the part of wave energy going over the ice floe surface cannot be effectively transmitted to downstream. Such dissipation becomes especially influential in wave-ice interactions, where overwash is ubiquitous because ice's freeboard is very small due to its close density to water. Consequently, T gets reduced and R + T would be considerably smaller than 1.

In such a context, ascertaining the energy dissipation due to overwash becomes important for wave-ice interaction; nonetheless, since the exclusion in previous theoretical models, overwash has been reported to be a key gap in this topic. This has been corroborated by the experiments of Yiew et al. [4] and Nelli et al. [5]. Particularly, they extracted the significant implication of overwash by building edge barriers on the upper surface of ice to prevent its occurrence, and then make comparisons between the experiments with and without the edge barriers – they shown theoretical models can accurately predict the process only when edge barriers are installed; by contrast, when there is no edge barrier, different extents of deviations were produced associated with different extents of overwash.

Due to the need of including overwash in the wave-ice modelling, there arise attempts to use the Computational Fluid Dynamics (CFD) method to simulate the process with high-order algorithms. Bai et al. [6], Huang & Thomas [7] and Nelli et al. [8] demonstrated that CFD can provide comparable results with corresponding experiments when overwash exists. However, CFD does not include solid mechanics, for which, the above examples assume ice to be rigid. This is only applicable when the ice dimension is relatively small to the incident wavelength. For a large ice floe, the rigid assumption becomes unrealistic as the ice starts to undertake elastic deformations, as presented in the experiments of Meylan et al. [9] and Sree et al. [10], which means the wave-ice interaction is actually a hydroelastic problem that may not be limited by the rigid scenario. More importantly, such deformations can influence the surrounding wave motion, thus changing R & T as well as the energy dissipation.

Therefore, another challenge is to include the hydroelastic effect in the process, which requires a set of additional structural solution of ice deformations and couple it with the CFD solution of surrounding fluid domain, i.e. a two-way Fluid-Structure Interaction (FSI) approach. As a solution, a two-way FSI scheme was developed by Tukovic et al. [11] under the opensource CFD framework, OpenFOAM [12], where the fluid and solid solutions are solved separately and fully coupled via the fluid-solid interface. This code was subsequently contributed by Cardiff et al. [13] with enhanced structural solutions, and by Huang [14] to enable free surface and ocean waves modelling. Following these efforts, Huang et al. [15] presented FSI simulations that have included both overwash and elastic effects in the wave-ice interaction and achieved good agreement with relevant experiments.

Up till this point, the developed OpenFOAM FSI solver is able to investigate the influences of overwash and elastic deformations on wave-ice interactions. Since previous research has put more emphasis on overwash, the present work aspires to analyse how can ice elasticity influence the interaction process. The Young's modulus (E) of ice will be varied from semi-rigid to realistic sea ice elasticities, based on experimental measurement values. Thus wave-ice interactions will be presented with the different E values, with particular attention on the associated variances in R & T and overwash to analyse energy dissipations. This work has the potential to facilitate the understanding in the wave-ice interaction by presenting the role of ice deformations.
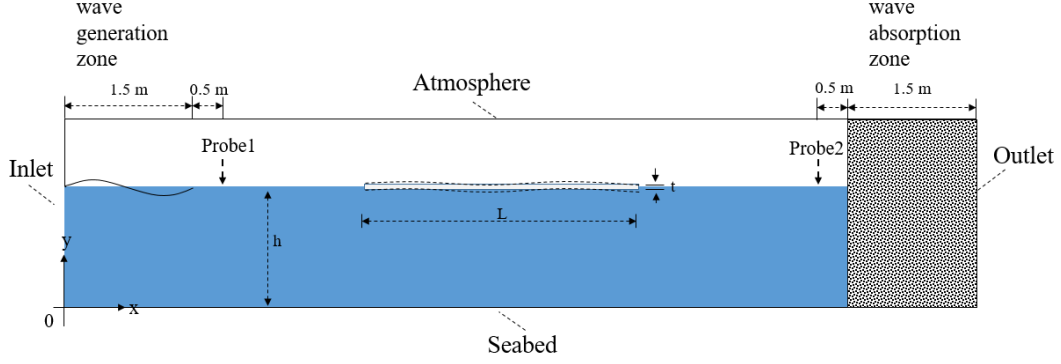
Figure 1: Schematic of the case: a thin ice floe is floating on the water surface and subjected to incoming waves, with its deformation induced.

2. Numerical Approach

In contrast to the traditional CFD approach that only solves governing equations for the fluid domain, the FSI approach requires the solutions of both the fluid and solid domains, alongside a coupling scheme to link the solutions together. To achieve this, the computational domain is divided into two parts, namely the fluid sub-domain and the solid sub-domain. A numerical wave tank is established in the fluid sub-domain to generate a regular wave field, and the solid sub-domain is a thin ice floe floating on the water surface. The case setup and solution process are presented as follows.

2.1 Computational domain and boundary conditions

As shown in Figure 1, a two-dimensional rectangular computational domain was assumed, defined by the Cartesian *x-y* coordinate system (indicated by 0 in Figure 1). The *x*-axis is parallel to the undisturbed water surface, and the *y*-axis is positive upwards. The computational domain (12 m long and 1.5 m high) is filled with fresh water to a depth of *h* with air filling the remainder of the fluid sub-domain. At the top boundary of the domain, a static pressure boundary condition is applied to represent atmospheric conditions. The bottom boundary is defined as a no-slip wall to account for the presence of the seabed. The solid sub-domain represents an ice floe of a high aspect ratio, floating on the water surface according to its buoyancy-gravity equilibrium position. The ice is fully flexible and not allowed to drift. The length and thickness of ice are denoted as *L* and *t* respectively.

Periodic regular waves were generated at the inlet boundary (left boundary of the domain), propagating in the positive *x*-direction, and a wave absorption zone was placed by the outlet boundary at the right of the domain to minimise reflection of waves. The wave generation and absorption were realised using the relaxation zone method implemented within the open-source wave toolbox, waves2Foam [16]. In the relaxation zone method, a spatial weighting factor χ is introduced. Along the positive direction of *x*-axis, χ increases from 0 to 1 in the wave generation zone and decreases from 1 to 0 in the wave absorption zone. A local field φ is dependent on χ as:

$$\phi = \chi\phi_{computed} + (1 - \chi)\phi_{target} \tag{1}$$

Thus, target results can be obtained at the inlet and outlet boundaries, where χ = 0, while fully computed results can be obtained between the two zones, where χ = 1. In the wave generation zone, the ϕ_{target} was defined as a regular wave field, according to the linear Stokes's wave theory [17],

$$\eta = h + \frac{H}{2}\cos(kx - \omega t) \tag{2}$$

$$u = \frac{\pi H}{\delta}\frac{\cosh k(y+h)}{\sinh kh}\cos(kx - \omega t) \tag{3}$$

$$v = \frac{\pi H}{\delta}\frac{\sinh k(y+h)}{\sinh kh}\sin(kx - \omega t) \tag{4}$$

in which η is the free surface elevation, *H* is the wave height (double of the wave amplitude *a*), δ is the wave period, *k* is the wavenumber and ω is the angular frequency. For the wave properties, *H* and δ are given in advance, and the wavelength ($\lambda = 2\pi/k$) was solved by the dispersion relation:

$$k\tanh kh = \kappa, \qquad \text{where} \quad \kappa = \omega^2/g \tag{5}$$

where *g* is gravitational acceleration set as 9.81 m/s². In the wave damping zone, the ϕ_{target} was set as still water, i.e. $\eta = h$ and *u = v = 0*. Two probes were positioned at upstream and downstream locations to record the time-varying free surface elevation.

2

2.2 Fluid-Structure Interaction

The partitioned FSI scheme of Tukovic et al. [11] is applied to couple the fluid and solid solutions, where the fluid and structural equations were solved separately and coupled at the fluid-solid interface. A Dirichlet-Neumann coupling procedure is employed, where velocity and pressure are first calculated in the fluid sub-domain, and the force at the fluid side of the interface is applied as a boundary condition to the solid side of the interface; the displacement in the solid sub-domain is then solved and the velocity at the solid side of the interface is applied as a boundary condition to the fluid side of the interface. Iterations are performed over these steps until the interface kinematic and dynamic conditions are satisfied, as illustrated in Figure 2. In this work, the fluid solution is obtained using the Navier-Stokes equations together with the Volume of Fluid (VOF) method, and the structural solution namely ice deformation is governed by the conservation of linear momentum, where the stress is given by the nonlinear St. Venant Kirchhoff hyperelastic law; details can be found in [15].

One advantage of the FSI method of the present work is that it employs the Finite Volume Method (FVM) [18] to discretise both fluid and solid domains. Most of current FSI works involve a combination of solvers, usually with an FVM solver for the fluid flow and another Finite-Element (FE) solver for the structural analysis, which requires a third code for coupling, data interpolation and simulation management. Therefore, such FV+FE approaches will tend to increase computational costs and impose limitations on the coupling method. This usually results in the simulation to be limited as one-way, i.e. FV fluid solutions are interpolated into the FE solver for structural analysis, while the deformed structure does not provide feedback to update the fluid solutions. In the wave-ice interaction, it is essential to consider the FSI to be two-way as the interest is to predict the changed wavefield with the presence of ice. On top of a two-way method, the coupling procedure has to go through sufficient iterations to satisfy the dynamic and kinetic conditions. As the entirely FVM approach of Tukovic et al. [11] is an all-in-one solver under the framework of OpenFOAM, it provides convenient management for the wave-ice coupling, thus suitable for modelling this case.
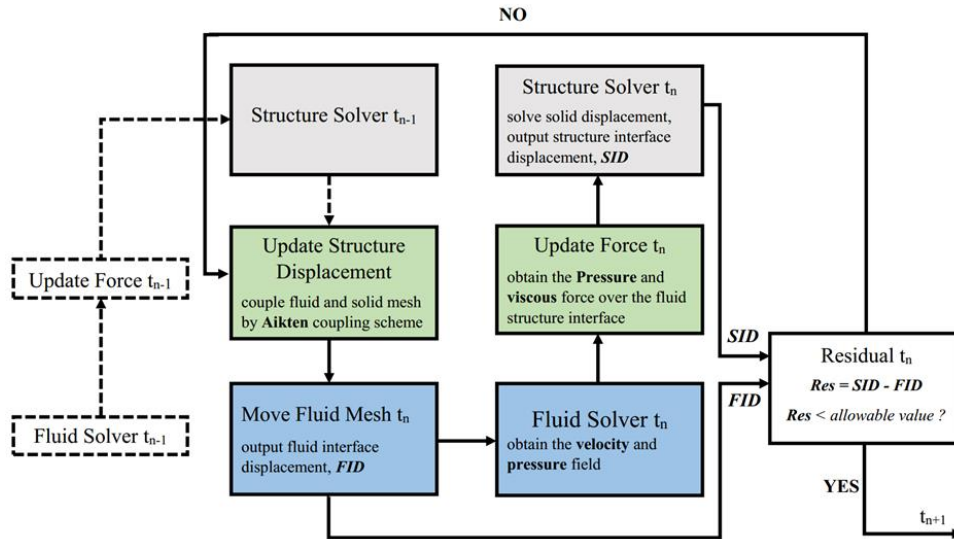

Figure 2: Flowchart of the FSI solution procedure.

2.3 Computational method

To obtain the fluid and structural solutions over a certain time duration, the process of FVM includes two types of discretisation, in space and time respectively. In space, the computational domain is divided into a set of non-overlapping hexahedral cells, known as a mesh; in time, the temporal dimension is split into a finite number of timesteps. As this is an FSI case, the computational mesh was divided into two parts, namely a fluid mesh for the fluid sub-domain and a solid mesh for the solid sub-domain, as shown in Figure 3. They are connected by placing their interface boundaries at the same location, where the fluid and solid interface meshes need not be conformal. The fluid mesh is graded towards the free surface area, while the solid mesh density is uniform. The cell numbers of both meshes were determined by sensitivity tests reported by Huang et al. [15]. Accordingly, the fluid mesh is made up of 100 cells per wavelength and 15 cells per wave height; the solid mesh consists of 100 cells per ice length and 4 cells per ice thickness. The size of each timestep was determined by a prescribed Courant number (Co) value, according to the expression:

$$Co = \frac{u\Delta t}{\Delta x} < 1 \qquad (6)$$

where Δt is the timestep size, $u/\Delta x$ is its normal velocity divided by the distance between the cell centre and the centre of the neighbour cell. Following the Co limit, Δt is set as 0.0005 s in this study. Using these spatial and temporal resolutions, the FSI model is able to accurately predict the wave-induced ice deformations, R & T, as well as overwash; relevant validations are presented in Huang et al. [15].
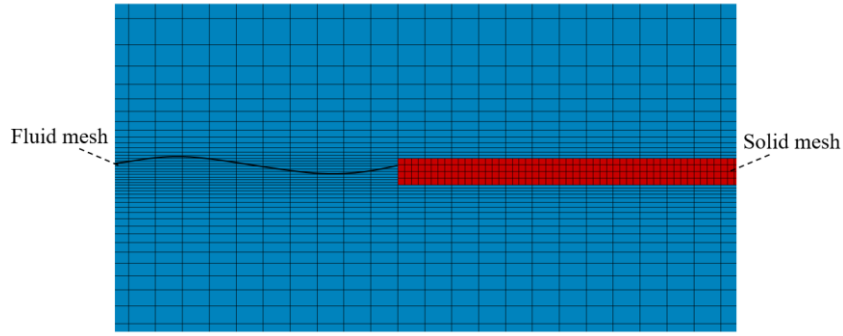
Figure 3: Mesh layout of the model: the fluid mesh density is graded towards the free surface area, while the solid mesh density is uniform.

3. Results and discussion

The Young's modulus of the ice model is varied to study its influence on the wave-ice interaction. The E values were selected according to a handful of experimental measurements. As Skene et al. [3] introduced, the E value close to a real sea ice floe is similar to that of a PVC material used by them, $E_1 = 500$ MPa. Apart from this, considering the highly regional and annual variance of sea ice, a range of E values are also tested in this case: $E_2 = 870$ MPa, a PP material used by Sree et al. [10]; $E_3 = 1.6$ GPa, another PP material used by Skene et al. [3]; $E_4 = 4$ GPa, fresh-water ice used by Dolatshah et al. [19], which is semi-rigid. Noting that these E values were measured on materials applied in model scale, they should be scaled when considered in full scale. The ice density is set at 900 kg/m^3, with $L = 1$ m and $t = 0.01$ m. The wave condition is set at $\delta = 0.9$ s, $\lambda = 1.26$ m, H = 0.032 m (ka = 0.08). This set of wave-ice conditions is selected because notable overwash will occur, as shown by Nelli et al. [5], thus the simulation can be as close to a realistic situation as possible.

Simulations were conducted using different E values and show notable differences in the results. Figure 4 provides a qualitative comparison between the wave interactions with semi-rigid and elastic ice. When the ice is semi-rigid, it conducts pitch motions induced by the incident waves; by contrast, when the ice is elastic, it tends to deform into the wave shape, fluctuating along with the surface wave. The latter agrees with the observation of Meylan et al. [9]. With different E values, the R & T as well as overwash depth were obtained after the ice has fully engaged in the periodic incident wave. To measure R & T, the free surface elevation measured by both probes in Figure 1 was analysed by a fast Fourier transform (FFT) to obtain the wave energy spectrum, and the wave energy was the integration of the energy spectrum over the frequency domain. Then T was calculated as the ratio of downstream wave energy to incident wave energy, while R is calculated as the ratio of the absolute difference between upstream wave energy and incident wave energy to incident wave energy, because the upstream wave is a superposition of the ice-reflected waves and the incident waves. The overwash depth was measured at the midpoint of the floe upper surface, taken average and denoted as $\overline{h_{ow}}$.

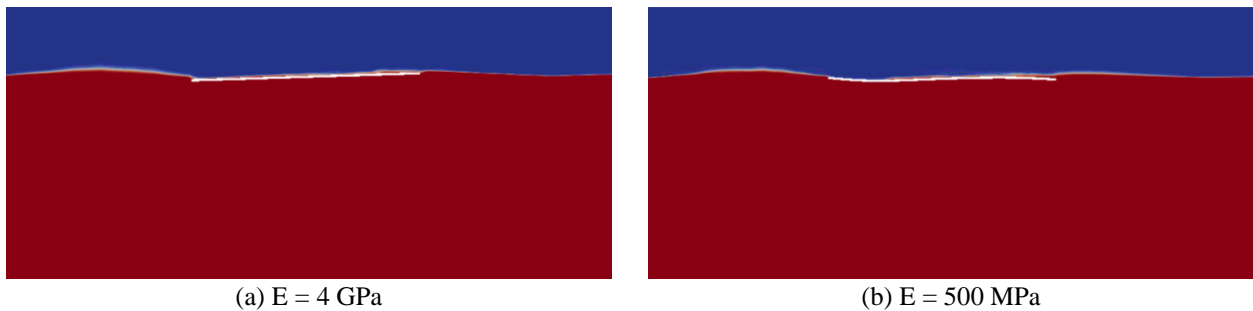(a) E = 4 GPa   (b) E = 500 MPa
Figure 4: Comparison of simulations between wave interactions with semi-rigid and elastic ice.

The R & T and $\overline{h_{ow}}$ obtained with different E values are listed in Table 1. It shows a clear trend that increasing E can produce lower T and higher R. T is the most significant parameter in the present topic, as it denotes how much of the incident wave energy can pass through the floe; it can then derive the attenuation of ocean waves in a multiple floes environment. The results show the waves will transmit better when the ice is more elastic; when a realistic sea ice elasticity is considered, it passes about 5% more energy than that when the ice is semi-rigid. This can be attributed to the behaviour that the elastic ice floe complies with the surface waves, as present in Figure 4(b), thus the wave feels less obstacle. R is slighter increased with an increased E, showing a more rigid floe will induce more reflection. However, the increase in R is less than the decrease of T, thus there is more energy dissipated with an increased E. In addition, the change in $\overline{h_{ow}}$ is very small (around 0.1 mm, 1% of the ice thickness) compare with the ice scale, thus the additional energy loss is unlikely due to overwash. It is thereby inferred that the additional energy dissipation is caused by additional vortical fluid behaviours due to the more rigid plate hitting the surrounding water. To prove this, the simulation can further analyse the vorticity of the fluid field, which has been included in the CFD solution.

Table 1: T, R and $\overline{h_{ow}}$ obtained with various E values.

E	500 MPa	870 MPa	1.6 GPa	4 GPa
T	0.821	0.815	0.802	0.778
R	0.097	0.106	0.109	0.112
$\overline{h_{ow}}$ (mm)	4.52	4.57	4.62	4.65

4. Conclusions

A fully coupling hydroelastic solver has been developed within the framework of OpenFOAM, by which, simulations of wave interactions with an elastic ice floe are presented, with a range of elasticity examined. This work demonstrates a realistically elastic sea ice floe can present a compliant behaviour to the incident surface wave, and it shows the importance to consider the elasticity since assuming the ice as rigid can cause additional energy loss of around 5%.

However, the present work has so far just conducted in a single wave condition. Intended future work is to examine the hydroelastic wave-ice interaction in a range of wave conditions. It has the potential to ascertain the magnitudes of R & T as well as energy dissipations due to different sources, mapped out against different incident wave conditions, which is a key gap for understanding the changing Arctic environment and improving current Polar-Earth climate models. In addition, the FSI approach can be further incorporated with an overset mesh technique to enable ice drift [20].

References

[1] L. G. Bennetts and T. D. Williams, 'Water wave transmission by an array of floating discs', in *Proceedings of the Royal Society of London A: Mathematical, Physical and Engineering Sciences*, 2015, vol. 471, p. 20140698.

[2] A. Toffoli *et al.*, 'Sea ice floes dissipate the energy of steep ocean waves', *Geophys. Res. Lett.*, vol. 42, no. 20, pp. 8547–8554, 2015.

[3] D. M. Skene, L. G. Bennetts, M. H. Meylan, and A. Toffoli, 'Modelling water wave overwash of a thin floating plate', *J. Fluid Mech.*, vol. 777, 2015.

[4] L. J. Yiew, L. G. Bennetts, M. H. Meylan, B. J. French, and G. A. Thomas, 'Hydrodynamic responses of a thin floating disk to regular waves', *Ocean Model.*, vol. 97, pp. 52–64, 2016.

[5] F. Nelli *et al.*, 'Reflection and transmission of regular water waves by a thin, floating plate', *Wave Motion*, vol. 70, pp. 209–221, 2017.

[6] W. Bai, T. Zhang, and D. J. McGovern, 'Response of small sea ice floes in regular waves: A comparison of numerical and experimental results', *Ocean Eng.*, vol. 129, pp. 495–506, 2017.

[7] L. Huang and G. Thomas, 'Simulation of Wave Interaction With a Circular Ice Floe', *J. Offshore Mech. Arct. Eng.*, vol. 141, no. 4, p. 041302, 2019.

[8] F. Nelli, L. G. Bennetts, D. M. Skene, and A. Toffoli, 'Water wave transmission and energy dissipation by a floating plate in the presence of overwash', *J. Fluid Mech.*, vol. 889, 2020.

[9] M. H. Meylan, L. G. Bennetts, C. Cavaliere, A. Alberello, and A. Toffoli, 'Experimental and theoretical models of wave-induced flexure of a sea ice floe', *Phys. Fluids*, vol. 27, no. 4, p. 041704, 2015.

[10] D. K. Sree, A. W.-K. Law, and H. H. Shen, 'An experimental study on gravity waves through a floating viscoelastic cover', *Cold Reg. Sci. Technol.*, vol. 155, pp. 289–299, 2018.

[11] Ž. Tuković, A. Karač, P. Cardiff, H. Jasak, and A. Ivanković, 'OpenFOAM Finite Volume Solver for Fluid-Solid Interaction', *Trans. FAMENA*, vol. 42, no. 3, pp. 1–31, Oct. 2018, doi: 10.21278/TOF.42301.

[12] H. Jasak, A. Jemcov, and Z. Tukovic, 'OpenFOAM: A C++ library for complex physics simulations', in *International workshop on coupled methods in numerical dynamics*, 2007, vol. 1000, pp. 1–20.

[13] P. Cardiff *et al.*, 'An open-source finite volume toolbox for solid mechanics and fluid-solid interaction simulations', *ArXiv Prepr. ArXiv180810736*, 2018.

[14] L. Huang, 'An opensource solver for wave-induced FSI problems', *Proc. CFD OpenSource Softw. Ed. Nilsson H*, 2018, doi: http://dx.doi.org/10.17196/OS_CFD#YEAR_2017.

[15] L. Huang, K. Ren, M. Li, Ž. Tuković, P. Cardiff, and G. Thomas, 'Fluid-structure interaction of a large ice sheet in waves', *Ocean Eng.*, vol. 182, pp. 102–111, 2019.

[16] N. G. Jacobsen, D. R. Fuhrman, and J. Fredsøe, 'A wave generation toolbox for the open-source CFD library: OpenFoam®', *Int. J. Numer. Methods Fluids*, vol. 70, no. 9, pp. 1073–1088, 2012.

[17] R. G. Dean and R. A. Dalrymple, *Water Wave Mechanics for Engineers and Scientists*, vol. 2. WORLD SCIENTIFIC, 1991.

[18] H. K. Versteeg and W. Malalasekera, *An introduction to computational fluid dynamics: the finite volume method*. Pearson Education, 2007.

[19] A. Dolatshah *et al.*, 'Hydroelastic interactions between water waves and floating freshwater ice', *Phys. Fluids*, vol. 30, no. 9, p. 091702, 2018.

[20] S. Tavakoli, F. Nelli, L. Bennetts, and A. Toffoli, 'Wave-induced drift of a thin floating plate: A numerical experiment', in *34th International Workshop on Water Waves and Floating Bodies (IWWWFB)*, 2019.